



Mass-Transfer Characteristics of Air- Suction Type Fermentors

Alaa K. M.

Genetic Engineering and Biotechnology Institute for Postgraduate Studies/ University of Baghdad
Iraq- Baghdad

(Received 17 February 2008; accepted 17 June 2008)

Abstract

Liquid-side mass-transfer coefficients ($K_L a$) were measured in air-suction type fermentors using physical absorption of oxygen. A fermentor of 0.5 m i.d. was used with a working capacity of 60 liters of liquid. Tap water was used as the liquid phase, and air was used as the gas phase. The bioreactor mixing system consists of shrouded-disk/curved-blade turbine with six evacuated bending blades. The effect of liquid submergence (S) was investigated. Further, the effects of the ratio of the impeller diameter (D) to the tank diameter (T), and the clearance of the impeller from the tank bottom (C) were also studied. The agitation speed (N) was varied in the range of 50-800 rpm. It was found that the value of $K_L a$ increased as the impeller diameter increased, while it was decreased continuously with increasing the clearance. The effect of impeller submergence on the value of mass transfer coefficient ($K_L a$) is not much pronounced.

Suitable correlation was developed for estimating mass transfer coefficient ($K_L a$) in this type of bioreactors.

$$\frac{K_L a}{N} = 5.3 \times 10^{-3} \text{Re}^{0.7} \text{Fr}^{0.36} \left(\frac{C}{D}\right)^{-0.23} \left(\frac{S}{D}\right)^{-0.012}$$

Keywords: Fermentors, Air–Suction Impeller, Mass Transfer Coefficient.

1. Introduction

The important functions of aeration in fermentors include oxygen transfer, liquid phase mixing to ensure oxygen availability in all parts of the contactor, and suspension of microorganisms. In addition to these applications, there are many reactions, such as hydrogenation, alkylation, oxidation, etc. During the past 30 years, substantial work has been reported on aerators in efforts to: (1) estimate the critical conditions for the onset of aeration, and (2) elucidate the effects of various parameters on the mass transfer rates (Fuchs, *et al.*, 1971), (Takase, *et al.*, 1984). There are two distinct regimes in the aeration process. At lower impeller speeds, the liquid surface is visually distinct, or bubbles are not present in the liquid. Under these conditions, mass transfer across the interface occurs by the mechanism of surface renewal by turbulent eddies in the liquid. At higher impeller speeds, larger eddies are formed near the interface, and these eddies can entrap bubbles by overcoming the resistance of

surface tension (Patil, *et al.*, 1999). The gas-liquid interface (a) available for mass transfer increases many fold as a result of turbulence aeration (Ognean, T. 1997). The intensity and frequency of the eddies depend on the tank geometry, the impeller geometry, the ratio of the impeller diameter to the tank diameter, the position of the impeller in the tank, the impeller speed, and the properties of the liquid such as its surface tension and viscosity (Matsumura, *et al.*, 1982). In the published literature, mass-transfer characteristics are reported for reactors with four-bladed Rushton turbine (Zlokarnik, 1979), van-disk turbine (Backharst *et al.*, 1998), radial impeller closed from bottom (Ognean, 1993). The effect of clearance and submergence on mass transfer coefficient was studied in surface aerator impeller (Patil, S. S. and Joshi, J. B., 2004). Effect of clearance between two impellers in a dual agitator was also investigated (Shukla, V. B. *et al.*, 2001). In multiple system the effect agitation speed on mass

transfer coefficient was investigated (Patil, S. S. and Joshi, J. B., 2003).

The aim of the present work is to study the effect of the impeller design parameter such as diameter, clearance, submergence, agitation speed on the mass transfer coefficient ($K_L a$).

2. Materials and Methods

Investigation was carried out in 0.5 m i.d. gas-inducing type of mechanically agitated reactor of 60 liter liquid capacity. The schematic diagrams of the bioreactor and the experimental setup are shown in Figure 1. The design details of vessel are given in Table 1. The prime mover was a DC motor, driven by a thyristor-controlled power source. The speed of rotation of the shaft was controlled by regulating the voltage applied to the armature of the motor by a ten-turn potentiometer. Fixed pulleys and twin C section were used to connect the agitator shaft to the motor. The entire device was able to control the speed. The bioreactor mixing system consists of shrouded-disk/curved-blade turbine with six evacuated bending blades as shown in Figure 2. The reactor tank, the central draft tube, the aeration wheel disk and hub were made of stainless steel. The air ducts were also stainless steel tubes, which were welded to the disk. The assembly was tinned and the hub was turned to fit a vulcanite sleeve in the bottom guide bearing. The shaft was made of $\frac{3}{4}$ inch stainless steel pipe. The cap for the introduction of air was bored to a tight running fit. Table (1) shows the dimensions of the agitated fermentor and the range of variables studied.

Table 1
Design Details of Gas-Inducing Mechanically Agitated Contactor.

Diameter of vessel, T	0.5 m
Impeller Diameter, D	T/3, T/5 (T=0.5 m)
Baffle width	10% of vessel diameter.
Number of baffles	4
Construction material	Stainless steel.
Geometry	Cylindrical with flat bottom
Lower impeller clearance from bottom, C	1.5D, 2D, 2.5D, 3D (D=9cm)
Submergence of upper impeller from the top liquid surface, S	0.5D, 1D, 1.5D. (D=15 cm).

The mass-transfer coefficient was measured by the unsteady-state oxygen absorption method. The tap water (at a temperature of 23-27°C) was deoxygenated by chemical reaction with sodium sulfite. A dissolved oxygen meter was used to measure the rate of oxygenation. The amount of dissolved sodium sulfite was too small to change mass-transfer properties of the water. The rate of oxygen transfer is given by

$$\frac{dC_m}{dt} = K_L a (C_m^* - C_m) \quad \dots(1)$$

(Patil, S. S. and Joshi, J. B., 2004).

where C_m is the dissolved oxygen concentration in the reactor at time t and C_m^* is the saturation concentration of oxygen in water in the reactor. The latter concentration was measured by allowing aeration to proceed until a constant value had been attained. Experiments on oxygen probes used in this work showed that the probes gave first-order responses, with time constants of around 5 seconds. The expression for this kind of probe can be written as

$$\frac{dC_p}{dt} = K_p (C_m - C_p) \quad \dots(2)$$

where C_p is the oxygen concentration measured by the probe and k_p is the probe constant. The values of the latter depend on the transport characteristics of the probe membrane, the nature of the electrolyte layer, and the electrochemical reaction at the cathode surface. We now introduce the following dimensionless quantities

$$X_p = \frac{C_p^* - C_p}{C_p^* - C_{p0}} \quad \dots(3)$$

$$X_m = \frac{C_m^* - C_m}{C_m^* - C_{m0}} \quad \dots(4)$$

Then, eqs 1 and 2 can be rewritten in dimensionless form as

$$\frac{dX_m}{dt} = -K_L a X_m \quad \dots(5)$$

$$\frac{dX_p}{dt} = K_p (X_m - X_p) \quad \dots(6)$$

In these expressions, C_{p0} and C_{m0} represent the concentrations of dissolved oxygen at time $t = 0$, and C_p^* represents the probe saturation concentration. Note that $C_{p0} = C_{m0}$ and $C_p^* = C_m^*$. Simultaneous solution of eqs 5 and 6 yields

$$X_p = \frac{K_p e^{-K_L a t} - K_L a e^{-K_p t}}{K_p - K_L a} \quad \dots(7)$$

The value of K_p , needed to solve eq. 7 for $K_L a$, can be determined from the probe response to a step input. For example, one could apply a

negative step input by transferring the probe from a container of water saturated with dissolved oxygen ($C_m=C_m^*$) to a container of oxygen-free sulfite solution ($C_m=0$) and noting the probe reading. For this case, eqs. 5 and 6 become

$$\frac{dC_p}{dt} = K_p (C_p^* - C_p) \quad \dots(8)$$

$$\frac{dX_p}{dt} = K_p X_p \quad \dots(9)$$

Eqs. 8 and 9 represent a special case of eqs 5 and 6 where X_m is replaced by X_p . K_p values for the probe were checked before and after each set of experiments. Variations in K_p values were not significant. From each aeration experiment, a set of values of $X_p(\text{actual})$ (called X_{pA}) was obtained as a function of time. By assuming a value of K_{La} , the value of X_p (equation) (X_{pE}) for a given time was calculated with eq 5. Then, the value of

the error for a given K_{La} and a given time was calculated according to

$$\text{Error} = \left(\frac{X_{pA} - X_{pE}}{X_{pA}} \right)^2 \quad \dots(10)$$

The value of K_{La} for given set of experiments was calculated by minimizing the total error (iterative calculation of above procedure) using the golden section optimization algorithm. The value of K_{La} was calculated with the assumption that the liquid phase was completely mixed. To confirm the liquid-phase mixing behavior, the oxygenation conditions (and hence K_{La}) were measured at different points (Figure 1): near the tank bottom (P-1); at the tank wall (P-2); and near the impeller (P-3); Gas was always dispersed at P-2 and P-3. It was observed that, the value of K_{La} was practically the same at all three points (Figure 3).

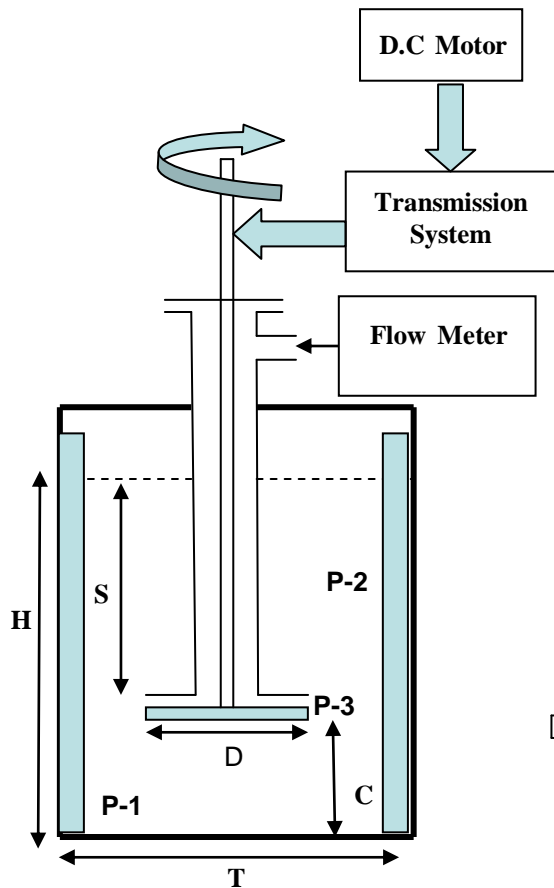


Fig.1. Schematic Diagram of the Experimental Diagram.

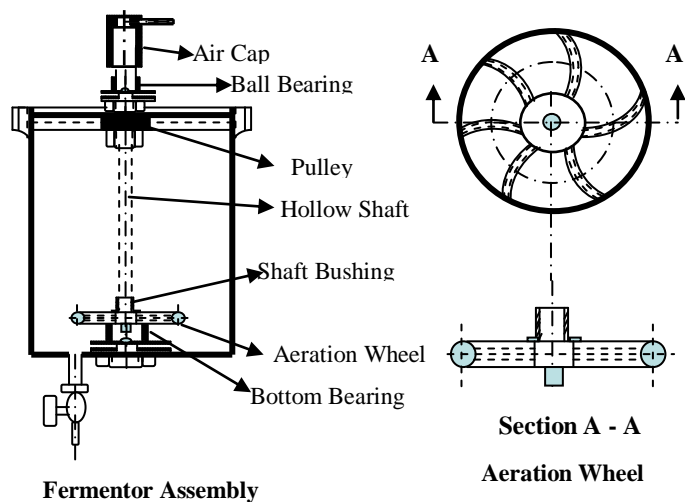


Fig. 2. Laboratory Experimental Fermentor with Mechanical Aerator.

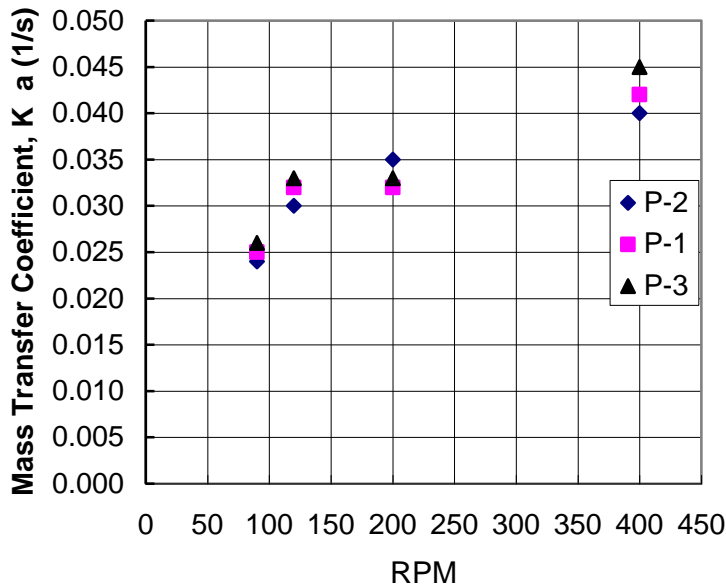


Fig. 3. Mass Transfer Coefficient at Different Prop Location;P-1 at Tank Bottom, P-2 at Tank Wall in the Impeller Plane, P-3 Near the Impeller.

3. Results and Discussion

3.1 Effect of Impeller Diameter

The effect of the impeller diameter D was studied with $D=T/3$ and $D=T/5$ impellers (Figure 4). In the lower range of RPM (<300), the $D=T/5$ impeller was found to exhibit relatively high values of $K_L a$. However, as the rpm increased beyond 300, the rate of increase in $K_L a$ with respect to rpm was diminished as a result of poor liquid circulation. This effect could be visually observed in terms of the gas dispersion characteristics. For $\text{rpm} > 300$, the gas hold-up in the top portion was found to increase with rpm but

the depth of gas dispersion was found to decrease and the value of $k_L a$ is nearly constant. The $K_L a$ values of the $D=T/3$ impeller were found to be higher. A similar trend was observed in the case of the surface aeration impeller (Patil, S. S.; Joshi, J. B. 2004). The effect of the impeller diameter was studied with $T/3$ and $T/5$ impellers. In the lower range of power consumption ($P/V < 100 \text{ W/m}^3$). The $T/5$ impeller was found to exhibit high values of $K_L a$. However, as the power consumption increased beyond 100 W/m^3 , the rate of increase in $K_L a$ with respect to P/V was diminished as a result of poor liquid circulation.

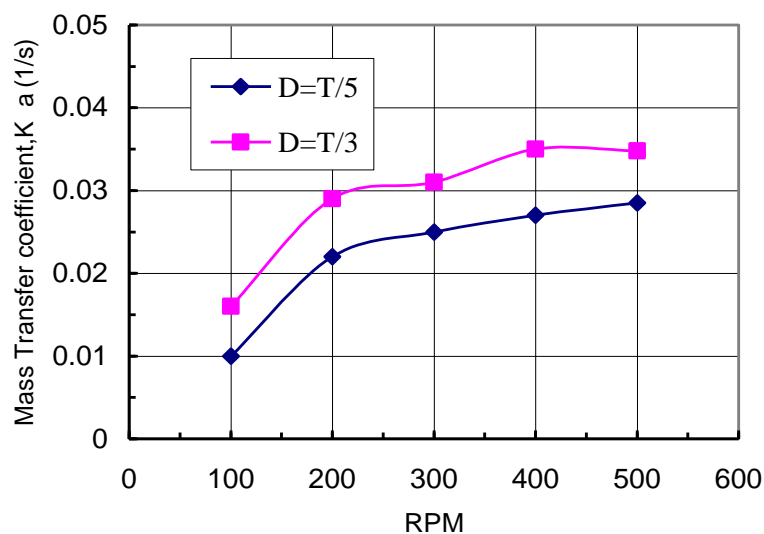


Fig. 4. Effect of Impeller Diameter (S=Just Submerged, $T=0.5 \text{ m}$, $C=1.5 D$).

3.2. Impeller Submergence

In the air-suction reactor, the stator protects the forced vortex, and irrespective of impeller submergence, the gas-liquid interface can approach very near to the impeller, especially at relatively high impeller speed at which bubble entrapment and subsequent transport become essentially independent of S . The effect of submergence was studied in the range: $S=0.5D$ to $S=2D$. From Figure (5), it can be seen that the effect of impeller submergence on the value of

mass transfer coefficient ($K_L a$) is not much pronounced. In the air suction impeller gas bubbles are entrapped into the surface waves and eddies formed by the impeller (Wu, H. 1995). With increasing submergence, the number of eddies at gas-liquid interface are decreased while the liquid circulation velocity increases with increasing submergence. The combined effect of bubble entrapment, and liquid circulation results in a nearly constant value of $K_L a$. with respect to S . Backhurst et al. (1998) made similar observations in the case of a vane-disk turbine.

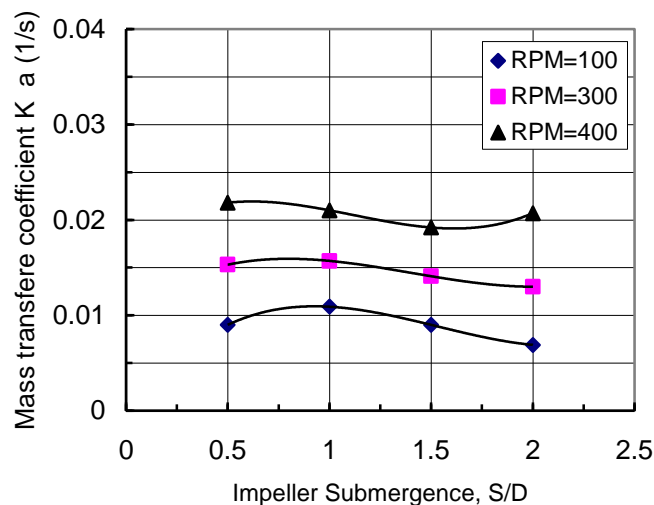


Fig. 5. Effect of Impeller Submergence on Mass Transfer Coefficient ($T=0.5$ m, $D=T/5$, $C=1.5D$).

3.4. Effect of Impeller Clearance

The effect of impeller clearance (C) at constant impeller submergence

(S) is shown in Figure (6). With the $D=T/5$ impeller diameter, the clearance was varied in the range of ($C=1.5D - C=3D$). The value of $K_L a$ was found to decrease continuously with increasing clearance. Increasing the clearance cause the region near the fermentor bottom to become a weak agitation or a dead zone region and hence the turbulence within the fluid decrease, the point which decreases the value of $K_L a$. Similar finding was observed by Patil, S. S. (2003) in studying the clearance in multiple impeller system.

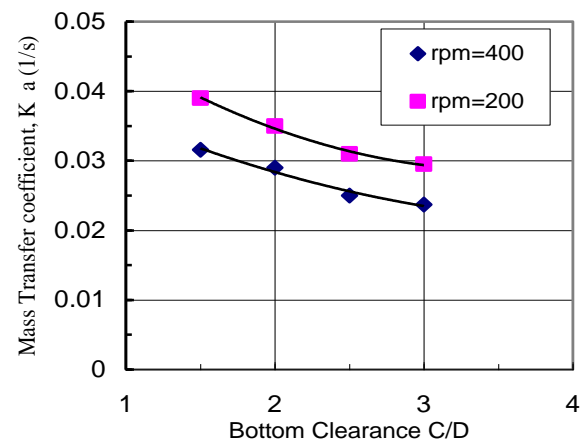


Fig. 6. Effect of Bottom Clearance on Mass Transfer Coefficient ($T=0.5$ m, $D=9$ cm, $S=1.5D$).

3.5. Mathematical Correlation

For establishing mathematical correlation between mass transfer coefficient ($K_L a$), and the variables studied : rotation speed (N), impeller bottom clearance (C), impeller submergence from top liquid level (S), the experimental data for this system were analysis using the multiregression method. Owing to the different variation of mass transfer coefficient ($K_L a$), the equation has been proposed is:

$$\frac{K_L a}{N} = 5.3 \times 10^{-3} \text{Re}^{0.7} \text{Fr}^{0.36} \left(\frac{C}{D}\right)^{-0.23} \left(\frac{S}{D}\right)^{-0.012} \dots (11)$$

Similar correlation was developed for estimating the mass transfer coefficient for multiple impeller system (Patil, S. S. and Joshi, J. B. 2003)

$$\frac{K_L a}{N} = 7 \times 10^{-6} N_p^{0.71} \text{Fr}^{0.48} \text{Re}^{0.82} \left(\frac{H}{D}\right)^{-0.54} \left(\frac{V}{D^3}\right)^{-1.08}$$

The parity plot shown in Figure 7. show that the correlation coefficient for above equation was found to be 0.96.

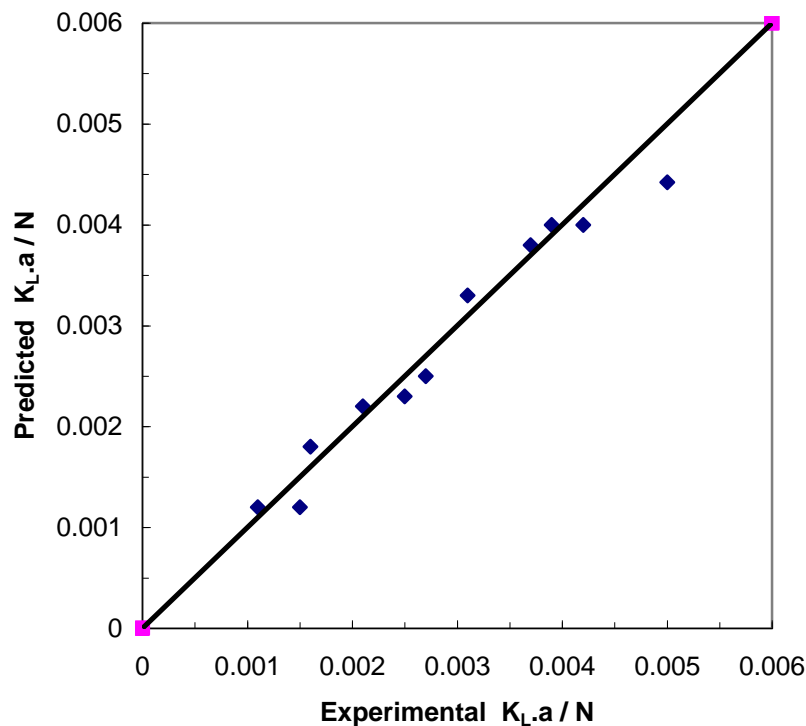


Fig. 7. Parity Plot of Mass-Transfer Correlation for Air-Suction Impeller (eq. 11).

4. Conclusions

- 1- The effect of the impeller diameter D was studied with $D = T/3$ and $D = T/5$ impellers. The $k_L a$ values of the $D = T/3$ impeller were found to be higher.
- 2- The effect of submergence (S) was studied in the range : $S = 0.5D$ to $S = 2D$. It can be seen that the effect of impeller submergence on the value of mass transfer coefficient ($K_L a$) is not much pronounced.

- 3- The effect of impeller clearance (C) at onstant impeller submergence (S) was studied in the range of ($C = 1.5D - C = 3D$). The value of $k_L a$ was found to decrease continuously with increasing clearance.
- 4- Mathematical correlation for estimating mass transfer coefficient ($K_L a$) has been proposed:

$$\frac{K_L a}{N} = 5.3 \times 10^{-3} \text{Re}^{0.7} \text{Fr}^{0.36} \left(\frac{C}{D}\right)^{-0.23} \left(\frac{S}{D}\right)^{-0.012}$$

5. Nomenclature

a	Interfacial area per unit volume (m ² /m ³).
C*	Saturated oxygen concentration, C _M * C _P * (g/L).
C _m	Oxygen concentration in the reactor (g/L).
C _m *	Saturated oxygen concentration in the reactor (g/L).
C _P	Oxygen concentration measured by probe (g/L).
C _P *	Saturated oxygen concentration measured by probe (g/L).
C ₀	Oxygen concentration at t = 0, C _{m0} , C _{P0} (g/L).
C	Impeller clearance from tank bottom (m).
D	Impeller diameter (m).
Fr	Froude number, N ² D/g.
g	Gravitational acceleration (m/s ²).
H	Liquid height (m).
k _L a	Mass-transfer coefficient (s ⁻¹).
k _P	probe constant (s ⁻¹).
N	Impeller speed (s ⁻¹).
N _P	impeller power number, (P/ρ N ³ D ⁵).
P	Power consumption (w)
Re	Reynolds number, ND ² ρ/μ
S	Impeller submergence (m)
T	Tank diameter (m)
t	Time (s)
V	Liquid volume in the reactor (m ³)
X _m	Dimensionless oxygen concentration in the reactor
X _P	Dimensionless oxygen concentration measured by probe
X _P *	Dimensionless saturated oxygen concentration
X _{PA}	Dimensionless actual oxygen concentration measured by probe
X _{PE}	Dimensionless equated oxygen concentration measured by probe
ρ	Liquid density. (Kg/m ³)
μ	Liquid viscosity. (Pa.s)

6. References

- Backhurst, J. R.; Harker, J. H.; Kaul, S. N.(1998) The Performance of Pilot and Full-Scale Vertical Shaft Aerators. *Water Res.*, 22, 1239.
- Fuchs, R.; Ryu, D. D.; Humphrey, A. E. (1971) Effect of Surface Aeration on Scale-up Procedures for Fermentation Process. *Ind. Eng. Chem. Process Des. Dev.*, 10, 190.
- Matsumura, M.; Sakuma, H.; Yamagata, T.; Kobayashi, J. (1982) Performance of Oxygen Transfer in a New Gas Entraining Fermentor. *J. Ferment. Technol.*, 60, 551.
- Ognean, T.(1993) Dimensionless Criteria for Estimating Oxygen Transfer in Aeration System. *Biotechnol. Bioeng.* , 41, 1014.
- Ognean, T. (1997) Relationship Between Oxygen Mass Transfer Rate and Power Consumption by Vertical Shaft Aerator. *WaterRes*, 31, 1332.
- Patil, S. S.; Joshi, J. B. (1999) Stability of Gas Inducing Type Impellers. *Can. J. Chem. Eng.*, 55, 793.
- Patil, S. S.; Joshi, J. B. (2004) Mass transfer characteristics of surface Aerators impellers. *Ind. Eng. Res.* 43, 2765.
- Patil, S. S.; Joshi, J. B. (2003) Optimum design of Multiple Impellers system. *Ind. Eng. Res.* 42,1261.
- Shukla, V.B.; Veera, U.P.; Kulkarni,P.R.; Pandit, A.B.(2001) Scale- up of bioreactor process in stirred tank reactor using dual impeller bioreactor. *Biochemical Engineering journal.* 8, 19.
- Takase, H.; Unno, H.; Akehata, T. (1984) Oxygen Transfer in a Surface Aeration Tank with Square Cross Section. *Int. Chem. Eng.*, 21, 128.
- Wu, H. (1995) An Issue on Applications on Applications of a Disk Turbine for Gas-Liquid Mass Transfer. *Chem. Eng. Sci.*, 50, 668.
- Zlokarnik, M. (1979) Scale-up of Surface Aerators for Wastewater Treatment. *Adv. Biochem. Eng.*, 11, 157.

خواص انتقال المادة في المخمرات ذات الخلاطات الساحبة للهواء

علاء كريم محمد

معهد الهندسة الوراثية والتقانات الاحيائية للدراسات العليا/جامعة بغداد

الخلاصة

تم حساب معامل انتقال المادة ($K_L a$) لذويان الاوكسجين في وسط سائل في نوع من المخمرات ذات الريش الساحبة للهواء (- Suction Air impeller). استخدم في هذا البحث مخمر اسطواني ذات قطر (0.5 م) وارتفاع (0.7 م) وسعة حجمية (60 لتر) سائل. استخدم ماء الحنفية كطور سائل، والهواء كطور غاز. الخلاط المستخدم من نوع الريش المنحنية المجوفة الساحبة للهواء (Shrouded-disk/curved-blade turbine with six evacuated bending blades) استخدمت في هذه الدراسة المتغيرات الاتية: سرعة دوران الخلاط (N)، قطر الخلاط المستخدم (D)، عمق الخلاط عن مستوى السطح العلوي لوسط السائل (S)، وارتفاع الخلاط عن قعر المخمر (C). وجد ان قيمة ($K_L a$) تزداد بازدياد قطر الخلاط، بينما تقل قيمته باستمرار زيادة ارتفاع الخلاط عن قعر المخمر (C). كذلك وجد عدم تأثير عمق الخلاط عن مستوى السطح العلوي لوسط السائل (S) على قيمة ($K_L a$). تم ربط هذه المتغيرات مع معامل انتقال المادة ($K_L a$) وفق معادلة تجريبية ذات مجاميع عديمة الوحدات (Dimensionless Groups):

$$\frac{K_L a}{N} = 5.3 \times 10^{-3} \text{Re}^{0.7} \text{Fr}^{0.36} \left(\frac{C}{D}\right)^{-0.23} \left(\frac{S}{D}\right)^{-0.012}$$